

Original Article

Electro-acupuncture (EA) mediated downregulation of microRNA-181a alleviates spinal cord neuronal apoptosis by inhibition of p38 MAPK pathway

Wei Chen, Yaochi Wu

Department of Acupuncture, Tuina and Traumatology, The Sixth People's Hospital Affiliated to Shanghai Jiaotong University, Shanghai, China

Received December 13, 2016; Accepted March 17, 2017; Epub May 15, 2017; Published May 30, 2017

Abstract: Spinal cord injury (SCI) is a major cause of long-term functional disability and has no clinically accepted treatment. Electro-acupuncture (EA), a traditional Chinese medical method, has been widely used for a range of neurological disorders, including SCI. Here, we sought to evaluate the role of EA to promote functional recoveries after SCI in rats and its molecular mechanisms. We firstly evaluated the therapeutic efficacy of EA in SCI model rats. Then we assessed the impact of EA on spinal cord neuronal apoptosis and examined activation of mitogen-activated protein kinases (MAPK) in spinal cord tissues of SCI rats by the terminal deoxynucleotidyl transferase dUTP nick end labeling (TUNEL) assay, immunohistochemistry and Western blot. Further, the miRNA expression patterns in spinal tissues of SCI rats before and after EA treatment was analyzed by microarray analysis and validated using quantitative real-time polymerase chain reaction (qRT-PCR). Finally, luciferase reporter assay was used to validate the correlation between miR-181a and MKP-5 in BV-2 cells. We demonstrated that EA significantly improved functional recovery of SCI rats. EA inhibited caspase-3 activation and alleviated cell apoptosis after SCI. We also found that the activation of p38 MAPK/iNOS pathway after SCI was significantly attenuated by EA. In addition, the microarray data revealed that a total of 43 differentially expressed miRNAs were regulated by EA. Among these miRNAs, miR-181a was one of the most dysregulated miRNAs after EA therapy and selected for further study. The anti-apoptotic role of EA-downregulated miR-181a was mediated by direct interaction with MAPK phosphatase-5 (MKP-5), a novel identified player involved in spinal cord cells apoptosis. Our results suggest that the neuroprotection by EA may be partly mediated via inhibition of p38 MAPK activation by regulating miR-181a in SCI rats. Thus, this study reports a novel mechanism for the clinical treatment of SCI using EA and opens up a novel avenue for treatment of SCI, especially by combining with drug therapy.

Keywords: Spinal cord injury (SCI), electro-acupuncture (EA), miR-181a, neuronal apoptosis, p38 MAPK

Introduction

Spinal cord injury is one of the most prevalent devastating injury observed in the central nervous system (CNS), which usually results in devastating neurological changes and disability [1]. Although great efforts have made to ameliorate functional outcome of patients with SCI, advances in therapy for this disease have been limited thus far. Therefore, it has been become imperative to search for novel therapeutic interventions of SCI.

Increasing evidence supports that acupuncture (AP) open up a novel avenue for treatment of numerous disorders, including analgesia, pain control, promotion of homeostasis and improvement in brain blood circulation [2-4]. Electro-

acupuncture (EA) is an effective method of acupuncture, and has been well documented that EA relieves neurological dysfunction in neurodegenerative disorders, such as Parkinson's disease (PD) and ischemia [5, 6]. Recent observations showed that EA at the acupoints of Governor Vessel (Du Meridian) and Jiaji (EX-B2) had an effectively therapeutic effect on treatment of SCI in rats [7]. In particular, a recent report shows that EA could inhibit neuronal apoptosis in the spinal cords of cats subjected to partial dorsal root ganglionectomy, possibly by Bax downregulation and Bcl-2 upregulation [8]. However, limited studies have pay attention on the underlying mechanisms of EA after SCI.

Based on these observations, we hypothesized that EA may exert neuroprotective effects after

SCI in rats. In the present study, we found that EA could improve locomotor function after SCI in part by inhibiting apoptotic cell death in the spinal cords of rats. Furthermore, we investigated the role of miR-181a on the anti-apoptotic effects of EA in SCI via inhibition of p38 MAPK pathway by targeting MAPK phosphatase-5 (MKP-5). The results of the present study may help to provide a new therapeutic target for the treatment of SCI.

Materials and methods

Cell culture and transfection

The immortalized murine BV-2 cell line was purchased from the Chinese Academy of Medical Science and cultured in DMEM/F12 (Hyclone, Waltham, MA, USA) supplemented with 10% fetal bovine serum (Hyclone), 100 U ml⁻¹ penicillin and streptomycin in 25-cm² culture flasks at 37°C in a humidified atmosphere with 5% CO₂. Then, miR-181a mimic, miR-181a inhibitor or miR negative control (Genepharma, Shanghai, China) were pre-incubated with Lipofectamine 2000 (Invitrogen) with the final concentration of miRNA analogs at 100 nmol l⁻¹.

Spinal cord injury

Adult male Sprague-Dawley rats (250-300 g) were purchased from the Animal Center of the Chinese Academy of Sciences. Rats were anesthetized with 10% chloral hydrate (3.5 mL/kg, i.p.). A laminectomy was carried out at the T9-T10 level, exposing the cord beneath without damaging the dura. The spinous processes of T8 and T11 were then clamped to stabilize the spine, and the exposed dorsal surface of the cord was subjected to contusion injury (10 g×25 mm) using a New York University impactor as previously reported [9]. For the sham-operated controls, the animals underwent a T10 laminectomy without weight-drop injury. All surgical interventions and postoperative animal care were performed in accordance with the Guidelines and Policies for Rodent Survival Surgery provided by the Animal Care Committee of the Shanghai Jiaotong University.

Electro-acupuncture stimulation procedure

Rats were randomly divided into two groups: a SCI group and an EA-treated (SCI-EA) group. For EA treatment, the rats were immobilized in wooden holders. Two needles were inserted

into the rostral-caudal sites of the injured spinal cord and were then connected to the output terminals of an electro-acupuncture apparatus (Model G6805-2A, Shanghai Huayi Medical Electronic Apparatus Company, China) and stimulated by continuous wave of 2 Hz frequency and 0.2 mA intensity for 30 minutes. EA was administered both at 2 hours and 8 hours of postsurgery.

Basso-Beattie-Bresnahan (BBB) tests

Locomotor activity was evaluated at 1, 3, 7, 14, 21, and 28 days post-injury using the BBB locomotion scale. Two independent and well-trained investigators who were blind as to the experimental conditions as described [10], observed the movement and scored the locomotor function according to the BBB scales. The final score of each animal was obtained by averaging the values from both investigators.

Tissue preparation

After SCI, animals were anesthetized with chloral hydrate and perfused via cardiac puncture initially with 0.1 M PBS (pH 7.4) and subsequently with 4% paraformaldehyde in 0.1 M phosphate buffer. A 20 mm section of the spinal cord, centered at the lesion site, was dissected out, post-fixed by immersion in the same fixative overnight and placed in 30% sucrose in 0.1 M PBS. The segment was embedded in OCT, and longitudinal or transverse sections were then cut at 10 or 16 µm.

TUNEL staining and immunohistochemistry

TUNEL was performed according to the instructions of the manufacturer (Oncor, Gaithersburg, MD) as described previously [11]. Briefly, slides, prepared as described, were washed with PBS three times, and incubated for 15 min at RT with a 20 µg/ml Proteinase K (Gibco BRL). The slides were rinsed twice times with PBS before being incubated in TUNEL reaction mixture for 60 min at 37°C. After rinsing with PBS three times for 3 min, sections were incubated with HRP-streptavidin reagent (1:200) in PBS for 30 min at RT.

For immunohistochemistry, cross sections centered within the injured part of the spinal cord segments were incubated with 3% H₂O₂ to eliminate endogenous peroxidase activity and then washed several times in phosphate-buffered

Electro-acupuncture and spinal cord neuronal apoptosis

saline. After incubating in 0.15% Triton X-100 at room temperature and blocking with 1% goat serum albumin in modified D-PBS Tween-20 for 1 h, the sections were incubated overnight with rabbit anti-caspase 3 antibody (1:200, Millipore). Next, sections were incubated with horseradish peroxidase-conjugated secondary antibody for 2 h. Diaminobenzidine served as the substrate for peroxidase.

MiRNA microarray assay

The microarray analysis for miRNA profiling was conducted by the miRCURY LNA Array system (Exiqon, Vedbaek, Denmark). Total RNA from 10 mm long segment of spinal cord prepared as described was extracted and purified, using the miRNeasy FFPE Kit (Qiagen, Hilden, Germany), following the manufacturer's instructions. Hybridization and scanning were performed according to the Affymetrix standard protocol, using Affymetrix® GeneChip™ Command Console software (AGCC). Discriminant miRNAs and differences between groups were analyzed using Bayes moderated t test (limma), with Benjamini Hochberg false discovery rate (FDR) at $P < 0.05$, unless otherwise specified. A cut-off of 2-fold change and $FDR < 0.05$ was applied to select up- and down-regulated miRNAs.

Quantitative real-time RT-PCR

Total RNA from 10 mm long segment of spinal cord prepared as described was extracted with TRIzol (Invitrogen, CA) according to manufacturer's instructions. Total RNA from each sample was reverse-transcribed to cDNA using the PrimeScript RT reagent Kit (TaKaRa, Tokyo, Japan) and qRT-PCR was performed using the SYBR Premix Ex Taq (TaKaRa, Tokyo, Japan) and miRNA-specific primers for three down-regulated (miR-511, miR-181a, and miR-572) and three up-regulated miRNA species (miR-378, miR-279, and miR-494). The relative microRNA levels were normalized to U6 expression for each sample. Analyses of gene expression were performed by the $2^{-\Delta\Delta Ct}$ method.

Western blot

Protein extracts (50 μ g) were separated by 12% SDS-PAGE and then transferred onto a PVDF membrane. After blocking non-specific binding sites with 5% skim milk in TBST (0.5% Tween 20 in TBS) for 1 h at room temperature, the mem-

branes were incubated with primary antibodies for phosphorylated MAPKs (p38 MAPK, MAPK-APK-2 and p-ERK) (1:1000 dilution; Cell Signaling Technology), iNOS (inducible Nitric Oxide Synthase) (1:400, Millipore, Bedford, MA, USA), cleaved caspase 3, cleaved caspase 9, cleaved PARP, (rabbit, 1:2000, Abcam, Cambridge, UK), caspase-3 (1:200), Bcl-2 (1:500), MKP-5 (rabbit, 1:1000, Santa Cruz Biotechnology), and β -actin (1:5000) overnight at 4°C. Finally, after washing, the membranes were treated with an HRP-conjugated secondary antibody (anti-rabbit, 1:5000, Jackson, USA) for 2 h at room temperature, and washed repeatedly. The protein bands were visualized by enhanced chemiluminescence detection reagents (ECL) (Applygen Technologies Inc., Beijing, China) as described in the manufacturer's instructions. Relative band intensities were determined by densitometry using Scion image software (version 4.0).

Luciferase reporter assay

A whole fragment of 3'UTR MKP-5 mRNA and a mutant form were cloned into pGL-3-Luc. The BV-2 cells were seeded in 12-well plates and co-transfected with pGL-3-MKP-5 wild-type or mutant portion and TK100 Renilla combined with miR-181a mimic, miR-181a inhibitor or each control, respectively, using Lipofectamine 2000 (Invitrogen). After 48 h of incubation, cells were collected for application in the Dual-Luciferase Reporter System (Promega, Madison, WI) following the manufacturer's recommendations. All of the dual-luciferase reporter assays were done in triplicate within each experiment, and three independent experiments were conducted.

Statistical analysis

Statistical analyses were performed with SPSS 13.0 software. The results were evaluated by χ^2 test and the other data were evaluated by Student's t-test and expressed as the mean \pm SD from three independent experiments. A *P*-value of less than 0.05 was considered statistically significant.

Results

Therapeutic efficacy of EA after SCI

The hindlimb movements were abolished immediately after SCI. A spontaneous functional recovery after SCI in both groups was observed.

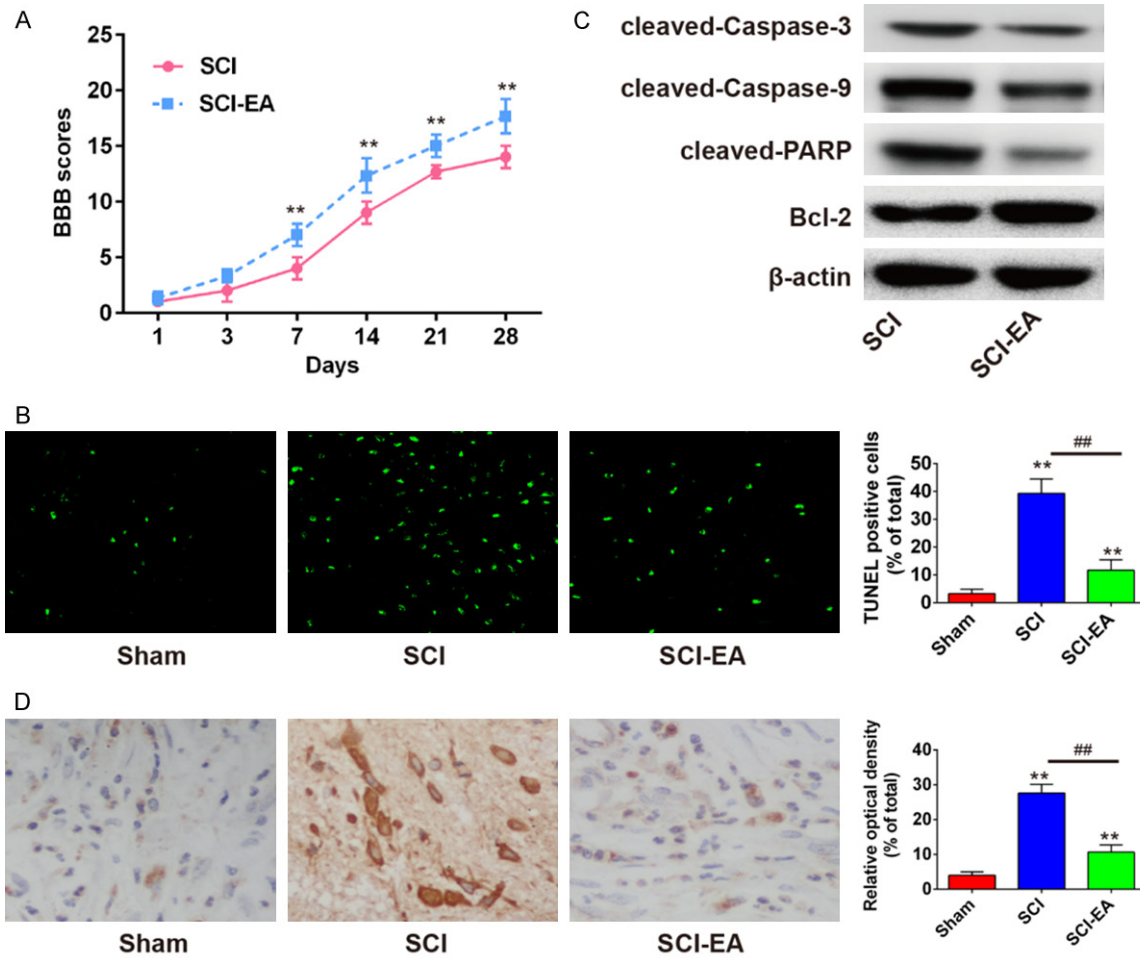


Figure 1. The therapeutic efficacy of EA after SCI. A. Hind limb locomotor function as assessed from day 1 to day 28 after SCI by BBB scores. Hindlimb dysfunction was relieved with treatment of EA (n=4) when compared with SCI group (n=4). **P<0.01 compared with the SCI group. B. Apoptosis was determined using TUNEL Staining. Cell with the TUNEL signal (green), which colocalized with DAPI (blue), were counted as apoptotic. EA significantly reduced the number of apoptotic cells after SCI. C. The levels of apoptosis-related proteins including cleaved caspases 3, cleaved 9, cleaved PARP and Bcl-2 are assessed by Western Blot after treatment with EA. D. Immunohistochemistry of cleaved-caspase-3. EA inhibits activation of caspase-3 after SCI. Data are presented as mean ± SD from three independent experiments.

As shown in **Figure 1A**, the rats in the SCI group gradually improved from Day 3, and rats in the SCI-EA group improved more rapidly. The statistical analysis showed a significantly greater increase in the BBB score from Day 7 to Day 28 in the SCI-EA group than in the SCI group, indicating that EA treatment could improve the movement of rats with SCI.

In recent years, apoptosis plays an important role of cell death in many neurological disorders including SCI. To determine whether EA could affect SCI-induced apoptosis, we performed TUNEL staining on spinal cord sections. The results showed that EA resulted in a mark-

ed reduction in the number of these cells compared with the SCI group (**Figure 1B**). Furthermore, we measured four apoptosis-related factors including cleaved caspase 3, cleaved caspase 9, cleaved PARP and Bcl-2. As shown in **Figure 1C**, the activated caspase-3, 9 and PARP were markedly decreased in the segment of spinal cord after EA treatment, which was along with upregulation of Bcl-2 protein. In the immunohistochemistry staining results, cleaved-caspase-3 positive cells in EA treated rats were dramatically decreased as compared with the SCI group, 7 days after injury, which was consistent with the results of Western Blot (**Figure 1D**). Our data suggested that EA treatment sig-

Electro-acupuncture and spinal cord neuronal apoptosis

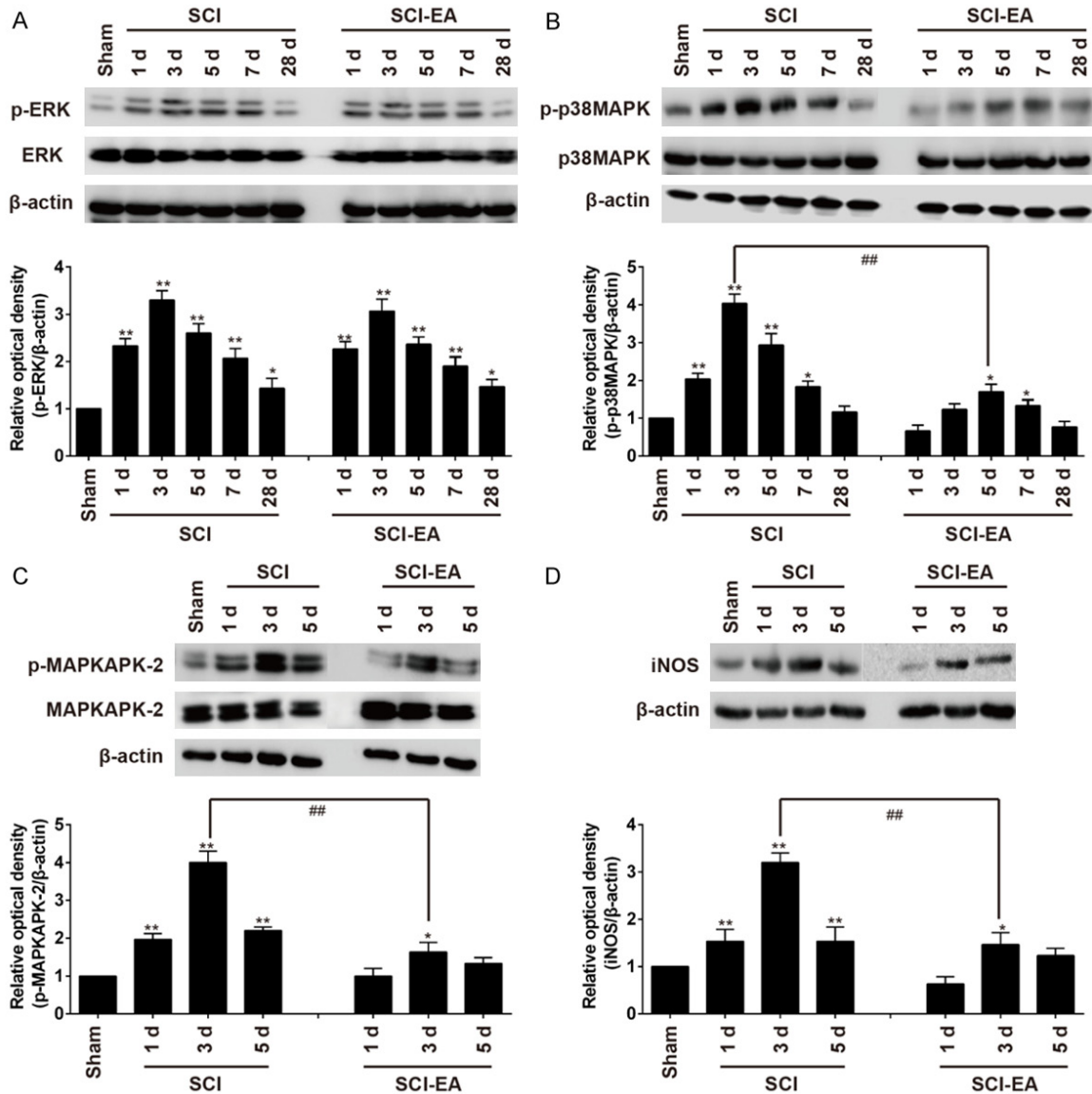


Figure 2. EA inhibits p38 MAPK/iNOS activation after SCI. Spinal cord tissue extracts were prepared as described in Materials and Methods (n=3). The gels presented are representative of results from three separate experiments. A. Western blot analysis of p-ERK. Quantitative analysis of Western blotting shows that EA treatment did not change the level of p-ERK compared with SCI group. B, C. Western blot detects the expression of p-p38 MAPK and p-MAPKAPK. Quantitative analysis of Western blotting shows that EA treatment significantly decreased the level of p-p38 MAPK and p-MAPKAPK compared with SCI group. D. Western blot analysis of iNOS. Quantitative analysis of Western blotting shows that EA treatment significantly decreased the level of iNOS compared with SCI group. Data are presented as mean \pm SD from three independent experiments. **P<0.01.

nificantly improves the SCI rat recovery in part through attenuating cell apoptosis.

EA inhibits the activation of p38 MAPK pathway after SCI

As the members of MAPK family, ERK and p38 MAPK pathway play key roles in apoptosis-related injury, we hypothesized that the protective

effect of EA in SCI recovery was partially through the activation of MAPKs pathway. There was a baseline phosphorylation of both ERK and p38 MAPK in the sham-operated group. After SCI, the levels of p-ERK and p-p38 MAPK were increased and peaked at 3 d, but the levels of them returned to baseline at 28 d following SCI because of the spontaneous functional recovery in SCI model rat (**Figure 2A, 2B**). How-

ever, after EA treatment, the level of p-ERK showed no significant difference among different time points between SCI group and EA-SCI group, but the level of p-p38 MAPK was significantly decreased (**Figure 2A** and **2B**). The activation of MAPKAPK-2, a downstream molecule of p38 MAPK, was also decreased after EA treatment (**Figure 2C**). These results suggest that EA attenuates the apoptosis after SCI through inhibiting p38 MAPK pathway, but not p-ERK pathway.

A recent study clearly demonstrates that activation of p38 MAPK can set in motion a cascade of iNOS expression followed by cell death programs that may participate in the injury process and exacerbate the initial injury [12]. Therefore, we examine whether EA attenuates the levels of iNOS. The results of Western blot analysis showed clearly that iNOS expression was significantly increased and peaked at 3 d in SCI group, compared with sham group. After EA treatment, the expression of iNOS was significantly decreased, compare with SCI group (**Figure 2D**). Collectively, these data showed that EA could attenuate the activation of p38 MAPK/iNOS pathway in SCI rats.

Aberrant expression of miRNAs after EA treatment in SCI

Increasing evidences support that microRNAs play indispensable roles in the pathophysiology of SCI [13]. To reveal miRNAs profiling response to EA therapy in rats, microarray analysis was performed to compare the miRNA expression profiles of medulla in rats treated with or without EA. According to the heatmap (**Figure 3A**), it was found that the expression levels of 43 miRs were dysregulated in the SCI-EA and SCI groups at 7 day, 14 day and 28 days after EA treatment, including 22 down-regulated miRNAs and 21 up-regulated miRNAs. To validate the microarray profiling data, qRT-PCR was used to confirm the expression of a subset of miRNAs including three down-regulated (miR-511, miR-181a, and miR-572) and three up-regulated miRNA species (miR-378, miR-279, and miR-494). The data showed that the expression of these miRNAs showed similar patterns as in the microarray analysis (**Figure 3B-G**). Among them, miR-181a was significantly down-regulated. In addition, because of its importance in the apoptosis, we concentrated our further experiments on miR-181a.

MKP-5 was the target gene of miR-181a

To explore the molecular mechanism of miR-181a, we performed a bioinformatics analysis using TargetScan and PicTar to predict potential target genes of miR-181a. The predicted binding sites for miR-181a in the mitogen-activated protein kinase phosphatase 5 (MKP-5) sequences are illustrated in **Figure 4A**. To validate whether MKP-5 is the direct target of miR-181a, a luciferase assay was performed with BV-2 cells as it is reported to share many characteristics with primary microglia [14, 15]. We generated luciferase reporter constructs by cloning either the wildtype or a mutated portion of the 3'UTR of MKP-5 into the 3'UTR of a pGL-3-Luc vector. We transfected these vectors with miR-181a mimic and miR-181a inhibitor into BV-2 cells and analyzed the lysates 48 h later. Transfection with miR-181a mimic markedly inhibited the luciferase activity for the wild-type 3'UTR of MKP-5 and transfection with miR-181a inhibitor promoted the luciferase activity, but both of them showed no repression effect for the mutated 3'UTR of MKP-5 when compared with that for the mimic or inhibitor control (**Figure 4B**), suggesting that miR-181a may repress MKP-5 expression by binding to the 3'UTR of MKP-5 in a direct and sequence-specific manner. In addition, western blot analysis showed that miR-181a overexpression decreased the levels of MKP-5 protein expression in BV-2 cells, whereas inhibition of miR-181a increased the expression of MKP-5 (**Figure 4C**). MiR-181a negatively regulates the expression of MKP-5 that deactivates MAPKs, suggesting that protective role of EA against SCI may be mediated in part via downregulating miR-181a expression by targeting MKP-5, inhibiting the activation of p38 MAPK.

Discussion

In the present study, we demonstrated that EA treatment improved functional recovery through inhibiting cell apoptosis after SCI in rats. Our results also showed that EA inhibited SCI-induced the activation of p38 MAPK/iNOS pathway via miR-181a. Taken together, our results indicate that microRNAs play an important role in EA treatment of SCI. More importantly, understanding the novel mechanism of action of EA will assist in the development of more potent and effective analogs for treatment of human SCI.

Electro-acupuncture and spinal cord neuronal apoptosis

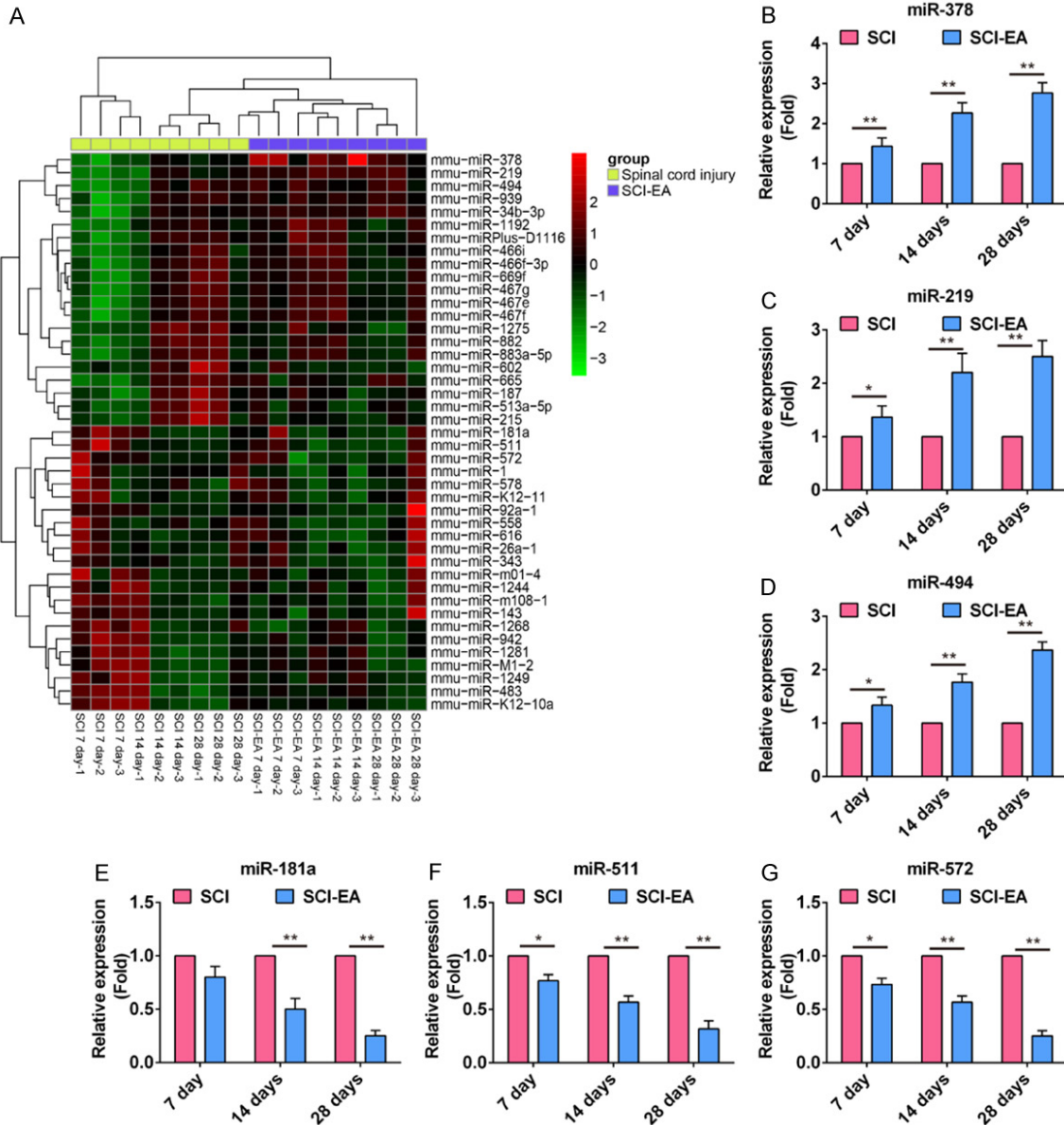


Figure 3. Hierarchical cluster analyses of altered microRNAs (miRNAs) after EA treatment. Differentially expressed miRNAs in the SCI and SCI-EA group, 7, 14 and 28 days day post-injury (n=3/group). A. Differentially expressed miRNAs in sham and SCI group 7, 14 and 28 days post-injury (n=3/group). Expression values are represented in shades of red and green indicating expression above and below the median expression value across all samples. B-G. qRT-PCR analysis confirmed the microarray analyses of six miRNAs (miR-378, miR-219 and miR-494, miR-181a, miR-511 and miR-572) at 7, 14 and 28 days after EA treatment. Data are presented as mean \pm SD from three independent experiments. *P<0.05, **P<0.01 vs. SCI group.

Apoptosis of neurons and oligodendrocytes after injury is a prominent feature of the secondary degenerative response, causing progressive degeneration of the spinal cord [16, 17]. Recent reports show that acupuncture is an effective therapeutic tool for recovery by inhibiting apoptosis after SCI [18]. More evidences have found that EA, an effective method of acupuncture, has been showed to attenuate isch-

emia-induced cerebral infarction and apoptosis [19-22]. And a study from Jiang H et al. showed that EA could inhibit neuronal apoptosis in MPTP-induced Parkinson's disease (PD) animal model, which indicate the potential neuroprotective effect of EA [23]. Our data reinforce this neuroprotective effects of EA by showing that the ability of EA to alleviate apoptotic cell death following SCI by inhibiting caspase-3 activation,

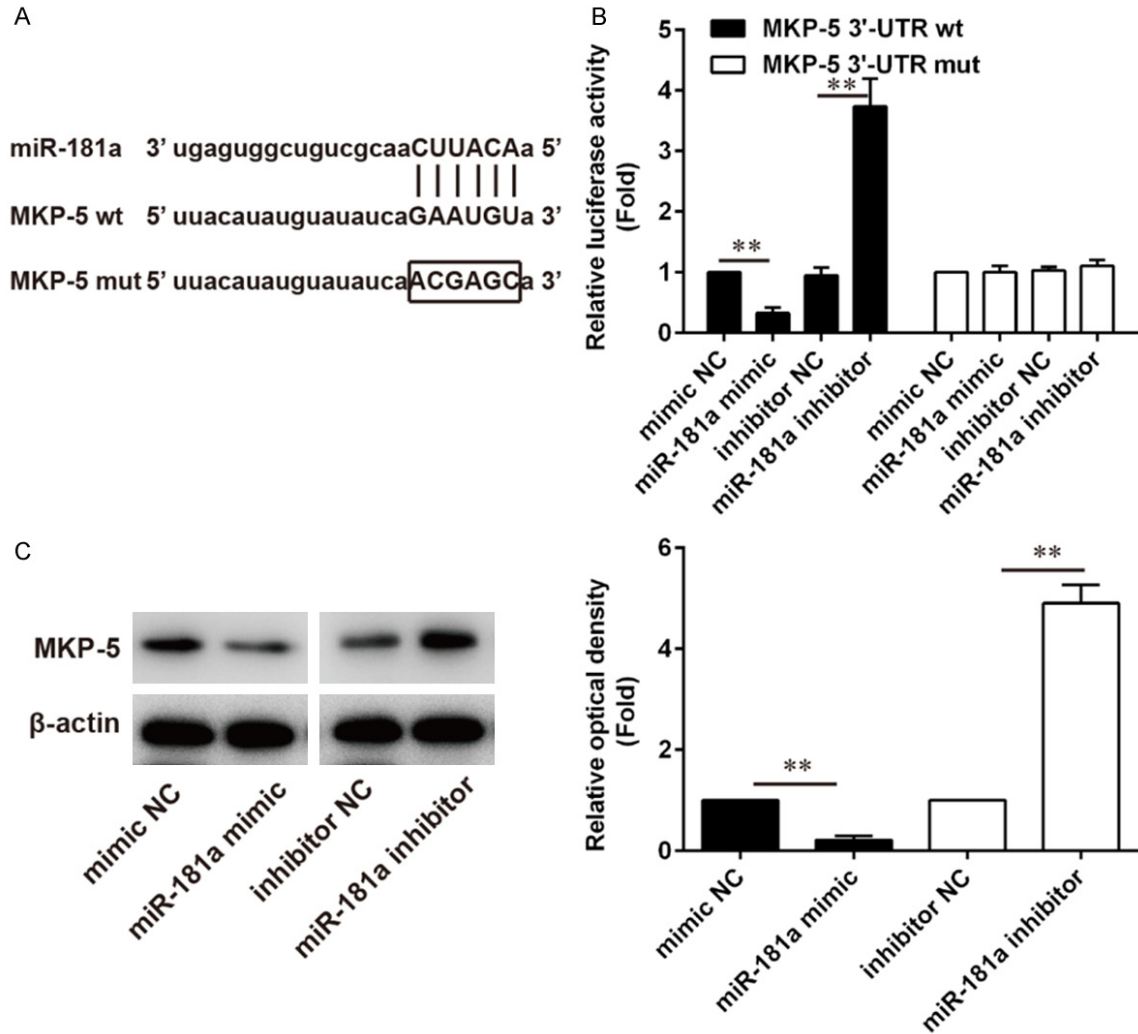


Figure 4. MKP-5 is a target of miR-181a. A. Schema of the firefly luciferase reporter constructs for the MKP-5, indicating the interaction sites between miR-181a and the 3'-UTRs of the MKP-5. B. Luciferase activities. Murine BV-2 cells were co-transfected with firefly luciferase constructs containing the MKP-5 wild-type or mutated 3'-UTRs and miR-181a mimic, mimic NC, miR-181a inhibitor or inhibitor NC, as indicated (n=3). C. The protein expression of MKP-5 after treatment with miR-181a mimic or miR-181a inhibitor (n=3). Data are presented as mean \pm SD from three independent experiments. **P<0.01 vs. inhibitor NC group or mimic NC group.

suggesting that EA could improve functional recovery through inhibiting cell apoptosis after SCI.

Increasing evidences show that SCI induces a marked activation of MAPKs including p38 MAPK, extracellular signal-regulated kinase [24] and c-Jun N-terminal kinase (JNK) in glial cells [25-27]. Because the p38 MAPK and ERK pathway are known to be associated with cell death or survival after SCI [9, 28] and we demonstrated that EA treatment after SCI inhibited apoptotic cell death of neurons and oligodendrocytes. Thus, we investigated whether EA treatment also modulate p38 MAPK and ERK pathway as well. Western blot analysis revealed

that the level of p-p38 MAPK was significantly decreased at 3 d to 28 d after EA treatment, but the level of p-ERK was not changed up to 28 d post-injury as previously reported elsewhere [29]. In addition, previous study showed that NO produced by iNOS was involved in induction of neuronal apoptosis following SCI. Our results also showed that iNOS expression was downregulated after EA treatment. Our results reveal that the EA-mediated cell apoptosis is in a p38 MAPK-independent manner.

The molecular mechanisms associated with SCI are very complicated. A variety of regulatory factors are involved in the pathogenesis of SCI including several miRNAs [30, 31]. MiRNAs

are endogenous, non-coding ~22 nt RNA molecules that negatively regulate gene expression at posttranscriptional level [32, 33]. Increasing evidence demonstrates that miRNAs are present in all systems, including the CNS, where they are involved in several neurological disorders such as Alzheimer's, Parkinson's, and Huntington's diseases, Tourette's syndrome and schizophrenia [34]. Preliminary studies have reported a variety of miRNAs abnormally expressed in SCI patients and animal models using microarray analysis [35, 36]. In this study, we performed a detailed analysis combining the use of microarrays and qPCR to characterize the microRNA expression changes in SCI-EA group in comparison with the SCI group at 3 different time points after EA treatment, and miR-181a was found significantly down-regulated in SCI-EA group. As the role of various miRNAs are being identified in the pathogenesis of SCI and p38 MAPK signaling pathway is known to play a crucial role in the development of SCI, we then investigated if p38 MAPK activity is associated with miR-181a regulation. In the present study, we found that miR-181a negatively regulates the expression of MKP-5 by directly binding to the 3'UTR, which is a critical negative regulator of MAPKs. EA treatment suppressed the induction of miR-181a by SCI, leading to the enhanced production of MKP-5 and subsequent inhibition of p38 MAPK. These preliminary results indicate that miR-181a is involved in the antiapoptotic effect of EA treatment in SCI model by inhibiting the activation of p38 MAPK pathway.

In summary, our findings demonstrated that EA provide effective therapeutic interventions for preventing the apoptotic death of oligodendrocytes and for improving functional recovery after SCI. Furthermore, our results reveal the mechanism of miR-181a/MKP-5/p38MAPK/iNOS axes involved in EA treatment of SCI and propose a potential pharmacological target for selective therapeutic intervention following SCI.

Acknowledgements

This work is supported by the 3-year Plan of Shanghai Traditional Chinese Medicine (No.: ZY3-JSFC-1-1008) and the Scientific Research Project of Shanghai Science and Technology Commission (No. 16401933900).

Disclosure of conflict of interest

None.

Address correspondence to: Yaochi Wu, Department of Acupuncture, Tuina and Traumatology, The Sixth People's Hospital Affiliated to Shanghai Jiaotong University, 600 Yishan Road, Shanghai 200-233, China. Tel: +86-21-24058567; E-mail: yaochiwu256@yeah.net

References

- [1] Ackery A, Tator C and Krassioukov A. A global perspective on spinal cord injury epidemiology. *J Neurotrauma* 2004; 21: 1355-1370.
- [2] Cheng PT, Wong MK and Chang PL. A therapeutic trial of acupuncture in neurogenic bladder of spinal cord injured patients-a preliminary report. *Spinal Cord* 1998; 36: 476-480.
- [3] Paola FA and Arnold M. Acupuncture and spinal cord medicine. *J Spinal Cord Med* 2003; 26: 12-20.
- [4] Dyson-Hudson TA, Kadar P, LaFontaine M, Emmons R, Kirshblum SC, Tulskey D and Komaroff E. Acupuncture for chronic shoulder pain in persons with spinal cord injury: a small-scale clinical trial. *Arch Phys Med Rehabil* 2007; 88: 1276-1283.
- [5] Chuang CM, Hsieh CL, Li TC and Lin JG. Acupuncture stimulation at Baihui acupoint reduced cerebral infarct and increased dopamine levels in chronic cerebral hypoperfusion and ischemia-reperfusion injured sprague-dawley rats. *Am J Chin Med* 2007; 35: 779-791.
- [6] Park HJ, Lee PH, Ahn YW, Choi YJ, Lee G, Lee DY, Chung ES and Jin BK. Neuroprotective effect of nicotine on dopaminergic neurons by anti-inflammatory action. *Eur J Neurosci* 2007; 26: 79-89.
- [7] Li WJ, Pan SQ, Zeng YS, Su BG, Li SM, Ding Y, Li Y and Ruan JW. Identification of acupuncture-specific proteins in the process of electro-acupuncture after spinal cord injury. *Neurosci Res* 2010; 67: 307-316.
- [8] Zhao W, Zhao Q, Liu J, Xu XY, Sun WW, Zhou X, Liu S and Wang TH. Electro-acupuncture reduces neuronal apoptosis linked to Bax and Bcl-2 expression in the spinal cords of cats subjected to partial dorsal root ganglionectomy. *Neurochem Res* 2008; 33: 2214-2221.
- [9] Yune TY, Lee JY, Jung GY, Kim SJ, Jiang MH, Kim YC, Oh YJ, Markelonis GJ and Oh TH. Minocycline alleviates death of oligodendrocytes by inhibiting pro-nerve growth factor production in microglia after spinal cord injury. *J Neurosci* 2007; 27: 7751-7761.
- [10] Basso DM, Beattie MS and Bresnahan JC. A sensitive and reliable locomotor rating scale for open field testing in rats. *J Neurotrauma* 1995; 12: 1-21.
- [11] Lee SM, Yune TY, Kim SJ, Kim YC, Oh YJ, Markelonis GJ and Oh TH. Minocycline inhibits

Electro-acupuncture and spinal cord neuronal apoptosis

- apoptotic cell death via attenuation of TNF- α expression following iNOS/NO induction by lipopolysaccharide in neuron/glia co-cultures. *J Neurochem* 2004; 91: 568-578.
- [12] Xu Z, Wang BR, Wang X, Kuang F, Duan XL, Jiao XY and Ju G. ERK1/2 and p38 mitogen-activated protein kinase mediate iNOS-induced spinal neuron degeneration after acute traumatic spinal cord injury. *Life Sci* 2006; 79: 1895-1905.
- [13] Hu JZ, Huang JH, Zeng L, Wang G, Cao M and Lu HB. Anti-apoptotic effect of microRNA-21 after contusion spinal cord injury in rats. *J Neurotrauma* 2013; 30: 1349-1360.
- [14] Yu DS, Lv G, Mei XF, Cao Y, Wang YF, Wang YS and Bi YL. MiR-200c regulates ROS-induced apoptosis in murine BV-2 cells by targeting FAP-1. *Spinal Cord* 2014; [Epub ahead of print].
- [15] Blasi E, Barluzzi R, Bocchini V, Mazzolla R and Bistoni F. immortalization of murine microglial cells by a v-raf/v-myc carrying retrovirus. *J Neuroimmunol* 1990; 27: 229-237.
- [16] Shuman SL, Bresnahan JC and Beattie MS. Apoptosis of microglia and oligodendrocytes after spinal cord contusion in rats. *J Neurosci Res* 1997; 50: 798-808.
- [17] Liu XZ, Xu XM, Hu R, Du C, Zhang SX, McDonald JW, Dong HX, Wu YJ, Fan GS, Jacquin MF, Hsu CY and Choi DW. Neuronal and glial apoptosis after traumatic spinal cord injury. *J Neurosci* 1997; 17: 5395-5406.
- [18] Choi DC, Lee JY, Moon YJ, Kim SW, Oh TH and Yune TY. Acupuncture-mediated inhibition of inflammation facilitates significant functional recovery after spinal cord injury. *Neurobiol Dis* 2010; 39: 272-282.
- [19] Guo J, Li R, Zhao P and Cheng J. Effect of taurine in combination with electroacupuncture on neuronal damage following transient focal cerebral ischemia in rats. *Acupunct Electrother Res* 2002; 27: 129-136.
- [20] Jang MH, Shin MC, Lee TH, Lim BV, Shin MS, Min BI, Kim H, Cho S, Kim EH and Kim CJ. Acupuncture suppresses ischemia-induced increase in c-Fos expression and apoptosis in the hippocampal CA1 region in gerbils. *Neurosci Lett* 2003; 347: 5-8.
- [21] Si QM, Wu GC and Cao XD. Effects of electroacupuncture on acute cerebral infarction. *Acupunct Electrother Res* 1998; 23: 117-124.
- [22] Yang WO, Huang YL, Da CD and Cheng JS. Electroacupuncture reduces rat's neuronal ischemic injury and enhances the expression of basic fibroblast growth factor. *Acupunct Electrother Res* 1999; 24: 1-10.
- [23] Jiang H, Li LJ, Wang J and Xie JX. Ghrelin antagonizes MPTP-induced neurotoxicity to the dopaminergic neurons in mouse substantia nigra. *Exp Neurol* 2008; 212: 532-537.
- [24] Kloosterman WP and Plasterk RH. The diverse functions of microRNAs in animal development and disease. *Dev Cell* 2006; 11: 441-450.
- [25] Jin SX, Zhuang ZY, Woolf CJ and Ji RR. p38 mitogen-activated protein kinase is activated after a spinal nerve ligation in spinal cord microglia and dorsal root ganglion neurons and contributes to the generation of neuropathic pain. *J Neurosci* 2003; 23: 4017-4022.
- [26] Ma W and Quirion R. Partial sciatic nerve ligation induces increase in the phosphorylation of extracellular signal-regulated kinase (ERK) and c-Jun N-terminal kinase (JNK) in astrocytes in the lumbar spinal dorsal horn and the gracile nucleus. *Pain* 2002; 99: 175-184.
- [27] Zhuang ZY, Gerner P, Woolf CJ and Ji RR. ERK is sequentially activated in neurons, microglia, and astrocytes by spinal nerve ligation and contributes to mechanical allodynia in this neuropathic pain model. *Pain* 2005; 114: 149-159.
- [28] Yune TY, Park HG, Lee JY and Oh TH. Estrogen-induced Bcl-2 expression after spinal cord injury is mediated through phosphoinositide-3-kinase/Akt-dependent CREB activation. *J Neurotrauma* 2008; 25: 1121-1131.
- [29] Lee JY, Chung H, Yoo YS, Oh YJ, Oh TH, Park S and Yune TY. Inhibition of apoptotic cell death by ghrelin improves functional recovery after spinal cord injury. *Endocrinology* 2010; 151: 3815-3826.
- [30] Bareyre FM and Schwab ME. Inflammation, degeneration and regeneration in the injured spinal cord: insights from DNA microarrays. *Trends Neurosci* 2003; 26: 555-563.
- [31] Di Giovanni S, Knobloch SM, Brandoli C, Aden SA, Hoffman EP and Faden AI. Gene profiling in spinal cord injury shows role of cell cycle in neuronal death. *Ann Neurol* 2003; 53: 454-468.
- [32] Kosik KS. The neuronal microRNA system. *Nat Rev Neurosci* 2006; 7: 911-920.
- [33] Krichevsky AM. MicroRNA profiling: from dark matter to white matter, or identifying new players in neurobiology. *ScientificWorldJournal* 2007; 7: 155-166.
- [34] Hutchison ER, Okun E and Mattson MP. The therapeutic potential of microRNAs in nervous system damage, degeneration, and repair. *Neuromolecular Med* 2009; 11: 153-161.
- [35] Nakanishi K, Nakasa T, Tanaka N, Ishikawa M, Yamada K, Yamasaki K, Kamei N, Izumi B, Adachi N, Miyaki S, Asahara H and Ochi M. Responses of microRNAs 124a and 223 following spinal cord injury in mice. *Spinal Cord* 2010; 48: 192-196.
- [36] Liu NK, Wang XF, Lu QB and Xu XM. Altered microRNA expression following traumatic spinal cord injury. *Exp Neurol* 2009; 219: 424-429.